Supporting Information

Kim et al. 10.1073/pnas.1403457111

SI Materials and Methods

Ribosomal Complexes Formation. $tRNA^{Lys}$ (ChemBlock; MP Biomedicals) was labeled at the natural modification of the 3-(3-amino-3-carboxypropyl)uridine at position 47 (acp3U47) with Cy5 NHS ester and purified with hydrophobic interaction chromatography on FPLC (1). tRNAs (MP Biomedicals; Sigma) were aminoacylated with DEAE-purified S-100 enzymes and purified by acid-saturated phenol-chloroform extractions (2). Initiation complex (IC) was enzymatically formed by incubating 1.2 μM 70S-L1(Cy3) with 2.5 μM initiation factors, 2.4 μM messenger RNA (mRNA), 2.5 μM $fMet\text{-}tRNA^{fMet}$, and 1 mM GTP in the Tris·polymix buffer [50 mM Tris·OAc (pH 7.5), 100 mM KCl, 5 mM NH_4OAc, 0.5 mM $Ca(OAc)_2$, 0.1 mM EDTA, 6 mM 2-mercaptoethanol, 5 mM putrescine, and 1 mM spermidine] at 10 mM $Mg(OAc)_2$. One round of translational elongation was carried out by incubating the 120 nM IC with preformed 1 μM ternary complex of EF-Tu(GTP)·Val-$tRNA^{Val}$ [TC(V)] and 2 μM GTP-bound elongation factor-G [EF-G(GTP)] at 37 °C to form posttranslocation complexes with fMet-Val-$tRNA^{Val}$ in the peptidyl-tRNA–binding (P) site (POST-V). Biotinylated DNA primer (5′-AAG TTA AAC AAA ATT ATT TCT AGA ATTTG-Biotin-3′, underlined nucleotides base-paired with mRNA) was coincubated to be annealed to the 5′ end of the mRNAs for surface immobilization.

Total Internal Reflection Fluorescence Microscopy. A laboratory-built objective-type, wide-field total internal reflection fluorescence (TIRF) microscope was used for single-molecule fluorescence resonance energy transfer (smFRET) measurements (3). It is equipped with an Olympus 100× UPlansApo (oil immersion, N.A. 1.4) objective lens, and an EMCCD (IXon $EM^{+}897$; Andor) as a detector. Excitation sources are a diode-pumped 532-nm laser (75 mW; CrystaLaser) for FRET measurements and He-Ne 633 nm (21 mW; Thorlabs, Inc.) for direct excitation of Cy5. Emissions are split into donor and acceptor channels by a laboratory-built multichannel imaging system and projected side-by-side on the EMCCD. The illuminated area on each channel is ∼50 × ∼25 μm with ∼100-nm pixel widths. Colocalization of molecules on both donor and acceptor channels and their time traces were obtained by using IDL (ITT) scripts (https://cplc.illinois.edu/software/, University of Illinois at Urbana–Champaign). Further data analysis was carried out using Matlab (MathWorks). Time resolutions of 50 and 100 ms were used at different excitation powers to maintain relatively high signal-to-background ratios.

Data Analysis. Time traces undergoing single-step photobleaching events or displaying intensities from single molecules were selected for further analysis. The FRET efficiency (E_{FRET}) is calculated as the acceptor fluorescence intensity divided by the sum of acceptor and donor fluorescence intensity after background subtraction and cross-talk corrections (0.14) for donor bleed-through to the acceptor channel. Time traces of fluctuating E_{FRET} signals were idealized by a hidden Markov modeling-based software (vbFRET) (4). E_{FRET} changes less than 0.1 were not considered as transitions. Mean dwell times in the absence of EF-G with 50 ms time resolution are averages of three replicates and the errors are their standard deviations. All other mean dwell times are averages of mean dwells obtained by a block bootstrapping method; half of the traces were randomly selected and dwell times from the selected traces were fitted to either a single exponential or a Poisson distribution. This procedure was repeated 1,000 times and the average mean dwell time and its error were determined as the average and the standard deviation of the fitted rate constants from all of the 1,000 repeats. Fittings of the dwell time histograms were carried out using Microcal Origin 6.0.

SI Equations

For frameshifting mRNA (FSmRNA)-programmed pretranslocation (PRE_{FS}) complexes, translocation starts with a reversible equilibrium between the classical state (C) and the hybrid state (H). The H state reversibly binds EF-G to form the G state. This state then irreversibly forms an intermediate (I) state and translocates to the Post state, releasing the fluorophore-labeled tRNA from the tRNA exit (E) site. In our E_{FRET} traces, all H, G, and I states present the same high E_{FRET} state, and thus are not distinguishable. Solely to make the following analysis easier to understand we arbitrarily assigned the H, G, and I states to different E_{FRET} states as shown below.

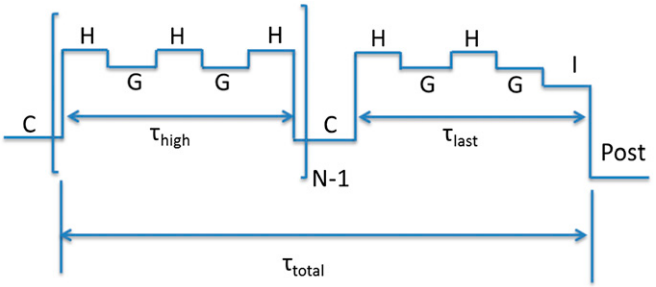

Our E_{FRET} trajectories (Fig. 2) show alternating periods of high E_{FRET} (states H, G, and I) and low E_{FRET} (state C) before complete translocation to the Post state with loss of acceptor fluorescence. Given a mechanism, in principle, all of the rate constants can be obtained from the measured dwell times (τ), and the branching ratios for species with multiple paths.

$$\tau_C = 1/k_{CH}$$
$$\tau_H = 1/(k_{HC} + k_{HG} \cdot [\text{EF-G}])$$
$$\tau_G = 1/(k_{GH} + k_{GI})$$
$$\tau_I = 1/k_{IP}$$

However, here we cannot measure individual dwell times for the species with indistinguishable E_{FRET} values (H, G, I). We can however easily obtain k_{CH} and k_{HC}. In the absence of EF-G, the E_{FRET} trace alternates between low and high E_{FRET}; the rate constants are the reciprocals of the measured dwell times. Thus,

$$k_{CH} = 1/\tau_C$$
$$k_{HC} = 1/\tau_{H0} = 1/\tau_H \quad \text{with} \quad [\text{EF-G}] = 0.$$

The k_{GI} is related to the n_{GH} and mean dwell time of the G state (τ_G), which are not measurable, therefore we can only approximately calculate the values of k_{GH} and k_{GI}. The approximation improves as the mean number of transitions to the high E_{FRET}

states per trajectory, N, increases (Table S1). For each trajectory the number of transitions is

$$n_{GI} = 1$$
$$n_{HG} = n_{GH} + 1$$
$$n_{HC} = N - 1.$$

Measurable quantities are the mean total time of the trajectories, τ_{total}; the mean number of transitions to the high E_{FRET} state including the last, N; and the mean times for the high E_{FRET} states before the last, τ_{high}; and the last E_{FRET} state, τ_{last}. They are related as follows:

$$\tau_{total} = n_C \cdot \tau_C + n_H \cdot \tau_H + n_G \cdot \tau_G + \tau_I = (N-1) \cdot \tau_{high} + (N-1) \cdot \tau_C + \tau_{last}$$
$$\tau_{last} = \tau_{high} - \tau_H + \tau_I$$

as $n_C = N - 1$,

$$N \cdot \tau_{high} = (n_H + 1) \cdot \tau_H + n_G \cdot \tau_G.$$

Using the branching ratios for transitions from states H and G, $k_{HG}[EF\text{-}G]/k_{HC}$ and k_{GH}/k_{GI}, we obtain the values for the number of states and their dwell times.

$$n_H = n_{HG} + N - 1$$
$$\tau_H = \tau_{H0} \cdot (N-1)/(n_{HG} + N - 1)$$
$$n_G = n_{HG}$$
$$\tau_G = 1/(k_{GI} \cdot n_{HG}).$$

Therefore

$$1/k_{GI} + (N-1) \cdot R \cdot \tau_{H0} = N \cdot \tau_{high}$$

with

$$R = (n_{HG} + N)/(n_{HG} + N - 1).$$

The values of N we measured varied from 1 to 3.4 (Fig. S7 and Table 1) with decreasing EF-G concentrations. There must be at least one H-to-G transition in each high E_{FRET} state, so n_{HG} is greater than or equal to N. R approaches 1 as N and n_{HG} increase; it is a maximum when they are minimum, thus

$$R_{max} = 2N/(2N-1), \quad R_{min} = 1.$$

Therefore,

$$k_{GI,max/min} = 1 \Big/ \left[N \cdot \tau_{high} - (N-1) \cdot R_{max/min} \cdot \tau_{H0}\right].$$

We calculated k_{GI} in the range of 0.20 to 0.48 s^{-1} from the experimental results of τ_{high} and N at 0.2, 0.5, and 1 μM EF-G (Table S1).

We can estimate lower and upper limits for k_{IP}

$$k_{IP} = 1 \Big/ \left[\tau_{last} - (\tau_{high} - \tau_H)\right]$$

so

$$1/\tau_{last} < k_{IP} < 1 \Big/ (\tau_{last} - \tau_{high}).$$

The estimated k_{IP} from the experimental results of τ_{last} and τ_{high} at 1 μM EF-G is ranged as; $0.16 \pm 0.03 < k_{IP} < 0.23 \pm 0.07$ (the errors are propagated errors).

1. Blanchard SC, Kim HD, Gonzalez RL, Jr., Puglisi JD, Chu S (2004) tRNA dynamics on the ribosome during translation. *Proc Natl Acad Sci USA* 101(35):12893–12898.
2. Moazed D, Noller HF (1989) Interaction of tRNA with 23S rRNA in the ribosomal A, P, and E sites. *Cell* 57(4):585–597.
3. Joo C, Ha T (2008) Single-molecule FRET with total internal reflection microscopy. *Single-Molecule Techniques: A Laboratory Manual*, eds Selvin PR, Ha T (Cold Spring Harbor Lab Press, Cold Spring Harbor, NY).
4. Bronson JE, Fei J, Hofman JM, Gonzalez RL, Jr., Wiggins CH (2009) Learning rates and states from biophysical time series: A Bayesian approach to model selection and single-molecule FRET data. *Biophys J* 97(12):3196–3205.

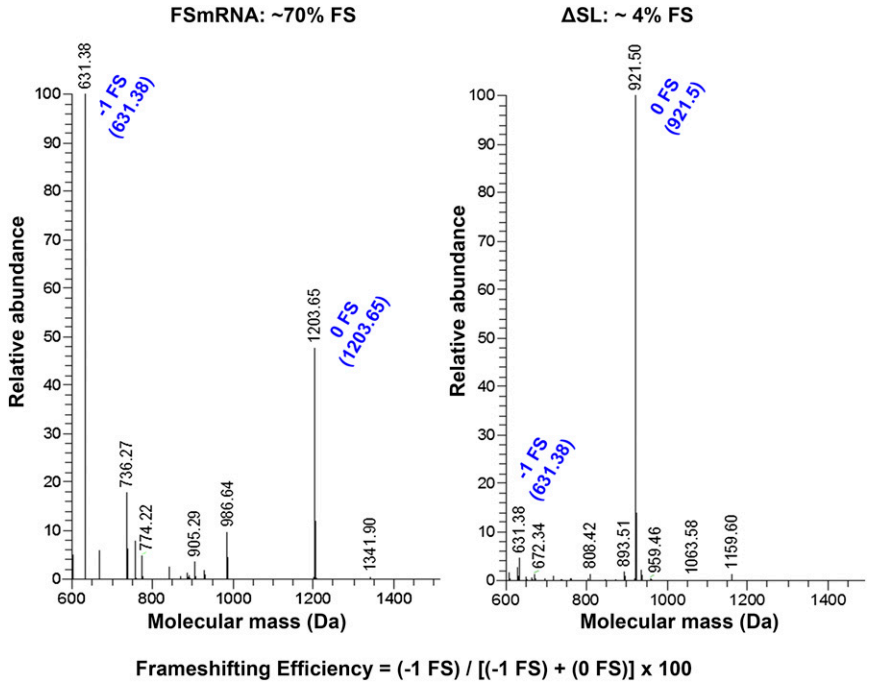

Fig. S1. LC–mass spectrometry analysis on in vitro translation products with FSmRNA (*Left*) or ΔSL (*Right*). Translations of the mRNAs were carried out using a reconstituted in vitro translation system (New England Biolabs) for 2 h at 37 °C, followed by 20 min incubation with 200 μM puromycin to release uncompleted polypeptide products from the ribosomal complexes. The products were purified by filtering with 100 kDa molecular cutoff filters (Millipore) and incubating in Ni-nitrilotriacetic acid agarose following the provided protocols, and subjected to LC–electrospray ionization mass spectrometry. Expected molecular masses for in-frame (0 FS) and −1 frameshifted (−1 FS) products are indicated in blue in parentheses. The results show ∼70% frameshifting efficiency for FSmRNA and ∼4% for ΔSL.

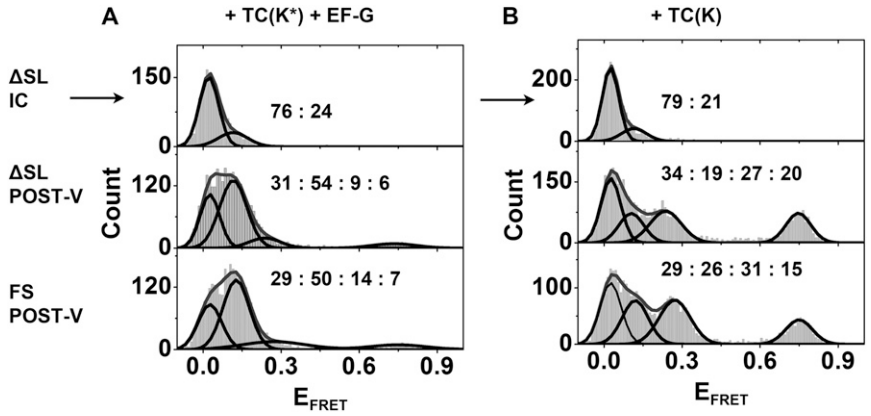

Fig. S2. Translation specificity and efficiency estimated from the averaged E_{FRET} histograms of molecules. (*A*) Immobilized ICs with ΔSL (*Top*), POST-V with ΔSL (*Middle*), and POST-V with FSmRNA (*Bottom*) were subjected to one round of elongation reaction by successive delivery of 100 nM TC(Cy5-K) and 2 μM EF-G (GTP) with washing steps in between. E_{FRET} per molecule is obtained by averaging the first 10 frames per trace. Whereas ICs showed a major peak around 0, POST-V complexes of either ΔSL or FSmRNA showed another intense peak at ∼0.15, indicative of POST-(Cy5)K. The results indicate that TC(Cy5-K) selectively incorporated into POST-V, displaying a lysine codon in the aminoacyl-tRNA–binding (*A*) site, and developed low E_{FRET} with Cy3 on the L1 stalk. It did not react with ICs, displaying a valine codon in the A site. The peak area at ∼0.15 occupies about 50% of the molecules for both ΔSL and FSmRNA, meaning ∼50% of POST-V complexes went through one cycle of translational elongation on the surface and formed POST-(Cy5)K_1. A few traces (<5%) fluctuating between the two E_{FRET} states of ∼0.2 and ∼0.8 are attributed to the populations at averaged E_{FRET} of ∼0.26 and ∼0.8 E_{FRET}. They are probably from the ribosomal complexes with spontaneously deacylated $tRNA^{Lys}$ in the P site causing them to fluctuate between the C (0.2 E_{FRET}) and H (0.8 E_{FRET}) states (1). Those traces were excluded during the analysis of the later step reactions. (*B*) Upon delivery of 250 nM TC(K) following the reaction in *A*, most of the IC molecules displayed E_{FRET} ∼0 and did not shift to the high E_{FRET} state (*Top*). However, about half of the population at ∼0.15 (*Middle* and *Bottom*) shifted to higher E_{FRET} of ∼0.26 and ∼0.8, indicating formation of PRE-(Cy5)K_1K_2 complexes. The low (∼0.26) and high (∼0.8) E_{FRET} states correspond to the C and H state of the PRE-(Cy5)K_1K_2 as demonstrated previously (1). The C state peak is shifted to slightly higher E_{FRET} (0.26 versus 0.2 in Fig. S3) due to the averaged values between the low and high E_{FRET} states. The results show ∼50% translation efficiency per each round of elongation on the surface for both ΔSL and FSmRNA complexes.

1. Fei J, Kosuri P, MacDougall DD, Gonzalez RL, Jr. (2008) Coupling of ribosomal L1 stalk and tRNA dynamics during translation elongation. *Mol Cell* 30(3):348–359.

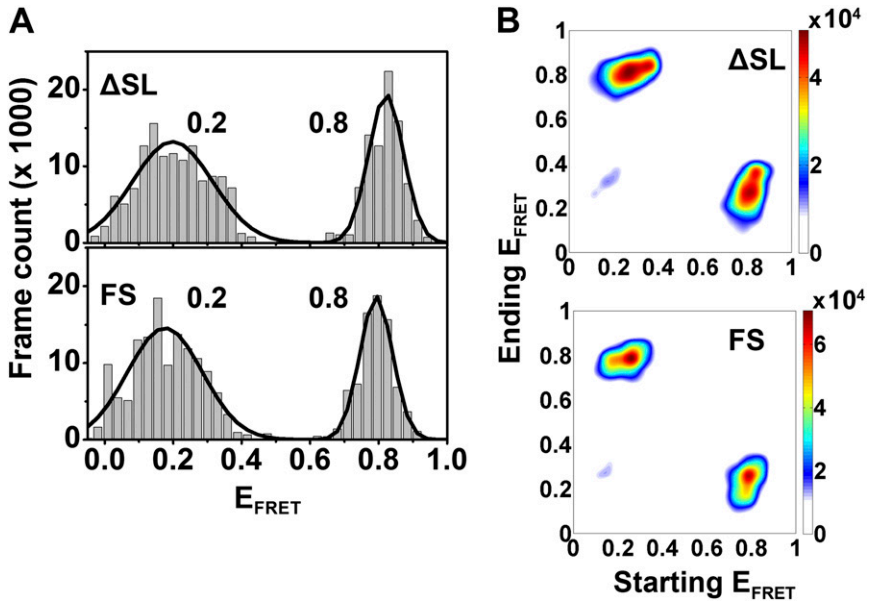

Fig. S3. (*A*) E_{FRET} histograms per frame of PRE-(Cy5)K_1K_2 complexes formed by delivering TC(K) in the absence of EF-G to POST-(Cy5)K_1 complexes. Molecules only showing fluctuation between low and high E_{FRET} states were selected to build the histograms. Fitting to Gaussian distributions showed two major peaks at 0.2 and 0.8 for both mRNA constructs. No significant difference was observed between the two mRNA constructs, indicating the downstream secondary structure does not affect the conformations probed by the current FRET pair. (*B*) Transition density plots of $PRE_{ΔSL}$ (*Upper*) and PRE_{FS} (*Lower*). Both plots show the reversible transitions between 0.2 and 0.8 E_{FRET} states. Time resolution was 50 ms per frame.

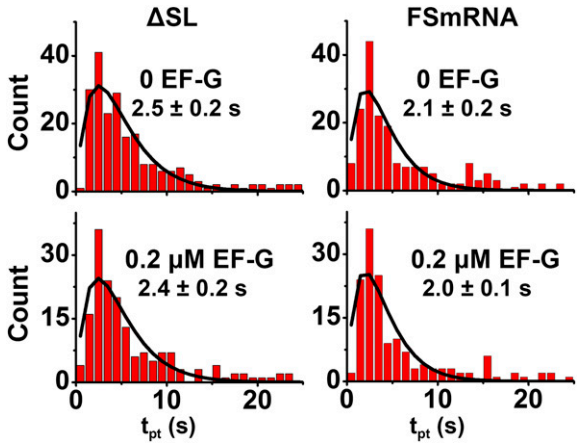

Fig. S4. Comparisons on $t_{pt,}$ duration measured from delivery of TC(K) to the first transition to the high E_{FRET} state for ΔSL (*Left*) and FSmRNA (*Right*). EF-G dependence was also examined with 0 (*Upper*) and 0.2 μM (*Lower*) EF-G(GTP). t_{tp} distributions were fitted to Poisson distributions with two rate-limiting steps ($y = A\ k^2\ te^{-kt}$). Time resolution was 50 ms per frame.

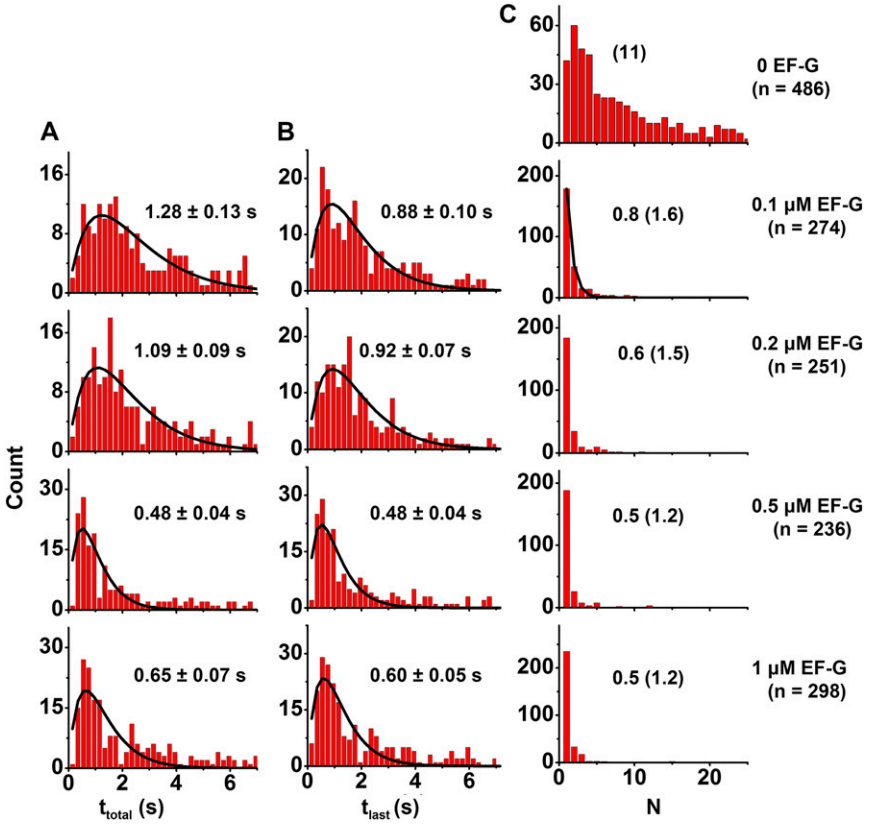

Fig. S5. Translocation of $PRE_{\Delta SL}$ in the presence of various EF-G(GTP) concentrations from 0 (*Top*) to 1 μM (*Bottom*). (*A*) t_{total} is the total duration from the first transition to the high E_{FRET} state until disappearance of Cy5 signals. (*B*) t_{last} is the dwell time of the last high E_{FRET} state. Both distributions were fitted by Poisson equations with two rate-limiting steps, $y = A\ k^2\ te^{-kt}$. Mean t_{total} (τ_{total}) were corrected for Cy5 photobleaching rate of 60 s using the equation of $1/\tau_{total} = 1/\tau_{total,obs} - 1/\tau_{photobleaching}$. Time resolution was 100 ms per frame. (*C*) The number of the transitions to the high E_{FRET} state per trace (N) distributions. Because 60–80% of $PRE_{\Delta SL}$ molecules translocate through a single transition to the high E_{FRET} state at 0.1–1 μM EF-G, fitting them with single exponential decay curves gave $N < 1$. In parentheses are the arithmetic average N for 95% of the populations.

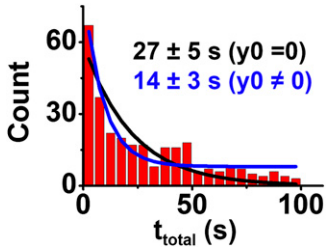

Fig. S6. t_{total} distributions of PRE_{FS} at 1 μM EF-G(GTP) with a time resolution of 100 ms per frame. The histogram was not well described by a single exponential decay curve. To estimate the mean value, the histogram was still fitted to single exponential decay curves with y_0 either fixed at zero (black) or as a variable (blue). After correction of the mean τ_{total} values for photobleaching rate of 60 s using the equation of $1/\tau_{total} = 1/\tau_{total,obs} - 1/\tau_{photobleaching}$, they became 49 ± 17 s or 18 ± 4 s, respectively.

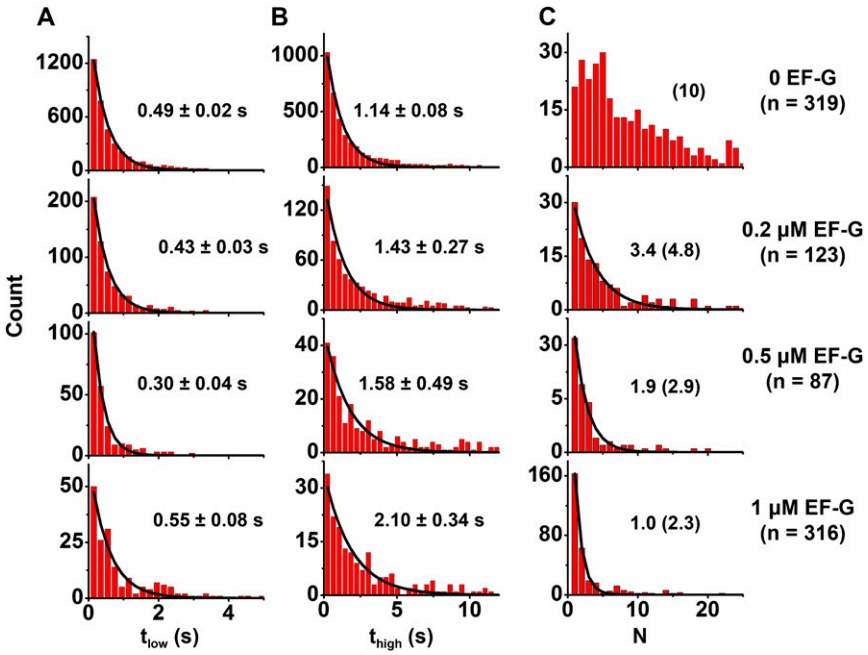

Fig. S7. Translocation of PRE_{FS} in the presence of various EF-G concentrations 0 (*Top*) to 1 μM (*Bottom*) observed with 100 ms per frame time resolution. Dwell time histograms of the (*A*) low and (*B*) high E_{FRET} state were well described by single exponential decay curves. (*C*) Histograms of the number of transitions to the high E_{FRET} state per trace (N) before the disappearance of the Cy5 signals. The mean N values were obtained from fitting to single exponential decay curves. Arithmetic average N for 95% of the populations are shown in the parentheses.

Table S1. Calculated G-to-I transition rate constants, k_{GI} for PRE_{FS}

	0.2 μM EF-G		0.5 μM EF-G		1 μM EF-G	
	N = 3.4 (4.8)		N = 1.9 (2.9)		N = 1 (2.3)	
n_{HG}/N	R	k_{GI}	R	k_{GI}	R	k_{GI}
1	1.2 (1.1)	0.29 (0.21)	1.4 (1.2)	0.42 (0.30)	2.0 (1.3)	0.48 (0.25)
2	1.1 (1.1)	0.29 (0.21)	1.2 (1.1)	0.41 (0.29)	1.5 (1.2)	0.48 (0.25)
3	1.1 (1.1)	0.28 (0.21)	1.2 (1.1)	0.41 (0.29)	1.3 (1.1)	0.48 (0.25)
>>10	1.0 (1.0)	0.28 (0.20)	1.0 (1.0)	0.39 (0.28)	1.0 (1.0)	0.48 (0.24)

Ranges of k_{GI} are obtained from the maximum and minimum R values. The values in parentheses were obtained by using arithmetic averages of N instead of values from the fittings (Table 1 and Fig. S7).